Simulación y Control

Revista Mexicana de Ingeniería Química
Vol. 14, No. 1 (2015) 149-165

ON THE DYNAMIC BEHAVIOUR OF A CLASS OF BIOREACTOR WITH NON-CONVENTIONAL YIELD COEFFICIENT FORM

SOBRE EL COMPORTAMIENTO DINÁMICO DE UN TIPO DE BIORREACTOR CON UN COEFICIENTE DE RENDIMIENTO NO CONVENCIONAL

R.V. Gómez-Acata[1], G. Lara-Cisneros[2], R. Femat[2], R. Aguilar-López[1*]

[1] *Departamento de Biotecnología y Bioingeniería, CINVESTAV-IPN, Av. Instituto Politécnico Nacional 2508, San Pedro Zacatenco, DF.*

[2] *División de Matemáticas Aplicadas, IPICYT, Camino a la Presa San José 2055, San Luis Potosí, S.L.P., México.*

Recibido 27 de Febrero de 2014; Aceptado 19 de Febrero de 2015

Abstract

The goal of this work is to analyze by numerical bifurcation the dynamical behavior of a class of continuous bioreactor used to hydrolyze cellulose using *Cellulomonas cellulans*, taking into account the effect of modeling the growth rate of this microorganism by six different kinetics models (monotonic and non-monotonic). Furthermore, it is considered that the biomass yield can be modeled as a constant or a variable case, for the variable case, a substrate dependent Gaussian-type function was proposed. The proposed non-conventional yield function is a realistic approach that describes the behavior of the cellular yield, unlike other models, this one is bounded to the maximum cellular yield and can be extrapolated to several operation conditions. Numerical results show changes in the equilibrium branches due to the kinetic growth model used. The non-conventional model of biomass yield produces a shift in the steady state multiplicity intervals, and new limit cycles were found with certain specific values of dilution rate and substrate feed.

Keywords: bifurcation analysis, continuous flow, limit cycle, local stability analysis, steady-state multiplicity, unstructured kinetic models.

Resumen

El objetivo de este trabajo es analizar mediante bifurcación numérica el comportamiento dinámico de una clase de biorreactor continuo, utilizado para la hidrólisis de carboximetilcelulosa por *Cellulomonas cellulans*, tomando en cuenta el efecto de modelar la velocidad de crecimiento de este microorganismo por seis diferentes modelos cinéticos no estructurados (monotónicos y no-monotónicos). En el análisis se considera que el rendimiento celular puede ser modelado como un valor constante o variable, para este último caso, fue propuesta una función tipo Gaussiana dependiente de la concentración de sustrato. El modelo para el rendimiento celular variable utilizado representa un enfoque más realista para describir el rendimiento celular, a diferencia de otros modelos reportados, la función es acotada al máximo rendimiento celular y puede ser extrapolado a diferentes condiciones de operación. Los resultados numéricos revelan cambios en las ramas de equilibrio debido al modelo de crecimiento utilizado. El modelo no convencional del coeficiente de rendimiento ocasiona un desplazamiento en los intervalos de multiplicidad de estados estacionarios, cambios en la estabilidad de los puntos de equilibrio y el surgimiento de ciclos límite a ciertos valores específicos de la tasa de dilución y de la concentración del sustrato de alimentación.

Palabras clave: análisis de bifurcación, flujo continuo, ciclo límite, análisis de estabilidad local, multiplicidad de estados estacionarios, modelos cinéticos no estructurados.

1 Introduction

The bioreactor mathematical models are employed to describe and predict the dynamics of its key state variables, such as metabolites, substrates and biomass concentrations. These models are also used in the design, optimization, on-line monitoring, and control of bioprocesses. To calculate the global rate for some biochemical reactions, that together transform at least one substrate to biomass and metabolites,

* *Corresponding author. E-mail*: : raguilar@cinvestav.mx

mass and energy balances have been formulated where the global rate is modeled frequently with logistic-type mathematical functions, known as unstructured growth models (Nielsen *et al*. 2003). In this way, the chemostat is the simplest bioreactor model that describes a microorganism culture (Fu & Ma, 2006), where a substrate is fed continuously into the bioreactor, which is consumed by the biomass and it is drawn off with the same input velocity. A minimum of two key states are regarded in a chemostat mass balance; the biomass and substrate concentrations (Dong & Ma, 2013). In spite of this relative simplicity, the chemostat is very useful in many biological and applied mathematical studies. Most of the previous theoretical studies have been-focused on understanding its dynamic behavior as stability, oscillations, steady state multiplicity and hysteresis to improve the bioprocess in which is involved (Garhyan *et al*. 2003; Abashar & Elnashaie, 2010), and to avoid falling into risky operation regions.

One of the earliest works focused in theoretical studies of chemostat model, was the stability analysis. It was conducted by Crooke *et al*. (1980), considering the Monod unstructured model and two biomass yield structures, constant and variable, the last one being as a linear increasing function that depends on the substrate concentration. The chemostat dynamic behavior with a constant biomass yield considering monotonic and non-monotonic growth rate has been analyzed in (Lara-Cisneros *et al*. 2012). The analysis showed that for the assumption of constant biomass yield, oscillatory behavior in the chemostat model is not possible, while the self-oscillations phenomenon occurred experimentally. On the other hand, if a linear biomass yield is considered, the oscillations are numerically possible. Similar results were obtained by Agrawal *et al*. (1982), they employed two different models, Monod and an unstructured inhibition, both with linear biomass yield. The linear biomass yield considers that the specific growth rate must increase and the specific substrate consumption rate must decrease fast enough with the substrate concentration. It is important to highlight that the biomass yield term has been considered constant for many *in silico* works, however, in practice this value is not constant along a fermentation process, because the microorganisms can be very sensitive to small changes on the culture media, for instance in temperature, oxygen dissolved, pressure, agitation, pH, inhibitory metabolites, etc.

Some other theoretical and numerical analysis for bioreactor models consider nonlinear models for the biomass yield, for instance in (Alvarez-Ramirez *et al*., 2009), where employing a variable biomass yield of the form $(A+BS)^n$ and the Monod model, implemented a linear substrate feedback control as a first stretch to eliminate oscillations with good results. In (Huang *et al*. 2007) is shown oscillatory behavior for a chemostat model with two microorganisms competing for one limiting substrate, where one microorganism was considered to have a constant biomass yield and the other with a nonlinear biomass yield of the form $(A+BS^n)$. On the other hand, in (Ibrahim *et al*. 2008), were taken into account the interactions between dissolved oxygen and the substrate in the continuous balance, a Monod-Haldane hybrid growth model, cell recycle, and the external mass transference resistance were set as modeling constrains, with this proposed study they found that periodic and chaotic behavior emerging at certain feed conditions and oxygen levels. In (Garhyan *et al*. 2003), a four-dimensional model of a *Zimomonas mobilis* fermentation was studied, considering the cell maintenance energy, an internal biomass key parameter, a second order polynomial for ethanol yield coefficient and the Monod growth model, the conditions for the oscillatory and chaotic behavior were found, employing the dilution rate and the substrate feed concentration as bifurcation parameters.

Many of the above works considered no inhibitions and used the Monod model, however, there are also analysis employing others unstructured models. For instance, Nelson & Sidhu (2008), taking the Tessier model and the linear biomass yield, they mentioned that natural oscillations can only occur if the feed substrate concentration is sufficiently high; Lenbury & Chiaranai (1987), studying a three variable system with a Levenspiel product inhibition model and linear biomass yield as a function of the product synthesis, they showed the existence of a periodic solution by theoretical analysis and simulation. In (Ajbar, 2001), considered the cell decay term, using the Haldane substrate inhibition model, and biomass attachment to the chemostat walls for the modelling. A complete analysis of the static and dynamic behavior of the above chemostat model for constant and linear biomass yield was made; Fu & Ma (2006), considering a simple chemostat model with a linear biomass yield term and Tissiet substrate inhibition model proved the existence of periodic solutions theoretically and by simulation.

Nevertheless, as far as we know, in literature there are few variable yield coefficient approaches, and the most models proposed are polynomial or exponential functions. The aim of this paper is to

analyze the dynamic behavior in a chemostat model considering the effect of a new biomass yield model (Gaussian function), as well as, different growth rate models (Aiba, Andrew, Haldane, Luong, Han-Levenspiel and Moser). The proposed variable yield coefficient model is a realistic approach to describe the behavior of the cellular yield, unlike other models, an important feature is that this model is bounded to the maximum cellular yield and can be extrapolated to several operation conditions. The analysis show rich dynamical behavior from multiplicity of equilibrium to different bifurcation types for the chemostat model with the proposed variable yield coefficient approach.

The manuscript has been structured as follows, the Section 2 shows the chemostat model for the hydroximethyl-cellulose hydrolysis; Section 3 addresses previous theory on local stability for the classic chemostat model; Section 4 has the results and discussion for the bifurcation analysis of the modified chemostat model. Finally, some concluding remarks are pointed out in Section 5.

2 Bioreactor model

Bioethanol production from cellulose hydrolysis is a promising alternative energy source, only a small percentage of all the microorganisms around the earth can degrade cellulose, mainly bacteria and fungi (Gupta *et al*., 2012). Only a handful of works relating to the mathematical modelling of cellulose hydrolysis by microorganisms are reported in literature, for example, Agarwal *et al*. (2009) calculated the value of the kinetic parameters for a set of growth kinetic models; all of these describe the carboxymethyl-cellulose hydrolysis by *Cellulomonas cellulans* in a batch culture. These growth models and its parameter values were taken for the development of this work (Table 1).

The chemostat model studied here, considers the biomass yield as a constant value or as a function of the substrate concentration. Some restrictions for the modelling are that it is bounded in the positive quadrant (mass concentrations cannot take negative values experimentally); is isothermal and homogeneous in the reactant concentrations in the entire vessel; no terms of death rate was considered and it is governed by the principle of mass conservation, PMC (Sterner, 2012).

From a mass balance for the substrate and biomass in the bioreactor, it is obtained the following system:

$$\frac{dS}{dt} = f(s,x) = DS_i - DS - \frac{\mu(S)X}{Y} \tag{1}$$

$$\frac{dX}{dt} = g(s,x) = -DX + \mu(S)X \tag{2}$$

Table 1. Unstructured growth models and their parameters obtained for a CMC hydrolysis by *Cellulomonas cellulans* in a bioreactor (Agarwal *et al*. 2009).

Model	*Equation*	Parameters
Aiba	$\mu = \mu max \frac{S}{(Ks+S)(1+S/Ki)}$	$\mu max = 0.383, Ks = 3.69, Ki = 6.569$
Andrew	$\mu = \mu max \frac{S}{(Ks+S)}\left(1-\frac{S}{S^*}\right)^n$	$\mu max = 0.412, Ks = 2.40, Ki = 2.5$
Haldane	$\mu = \mu max \frac{\left(1-\frac{S}{Cs}\right)^n S}{S+Ki\left(1-\frac{S}{Cs}\right)^m}$	$\mu max = 27.52, Ks = 388.3, Ki = 0.0256$
Han-Levenspiel	$\mu = \mu max \frac{S}{\left(Ks+S+S^2/Ki\right)}$	$\mu max = 0.182, S^* = 388.5, n = 42.27, m = 1202, Km = 544.6$
Luong	$\mu = \mu max \frac{S^n}{Ks+S^n}$	$\mu max = 0.385, Ks = 3.7, S^* = 103736, n = 15718$
Moser	$\mu = \mu max \frac{S}{Ks+S} e^{-S/Ki}$	$\mu max = 0.108, Ks = 0.0015, n = -2.66$

Table 2. Some expressions for the variable biomass yield.

Model	References
$Yxs(S) = Yo + Y1 \cdot S$	(Crooke, 1980), (Lenbury & Punpocha, 1989), (Lenbury & Chiaranai, 1987), (Ajbar, 2001);(Nelson & Sidhu, 2005),(Nelson, 2009);(Wu, 2007).
$Yxs(S) = (Ymin + a \cdot S)^p$	(Alvarez-Ramirez et al., 2009); (Wu, 2007)
$Yxs(S) = a + b \cdot S^2$	(Pilyugin, 2003); (Huang & Zhu, 2005)
$Yxs(S) = a + b \cdot S^3$	(Pilyugin, 2003)
$Yxs(S) = a + b \cdot S^m$	(Huang, Zhu, & Chang, 2007)
$Yxs(S) = a + b \cdot S + c \cdot S^2$	(Huang & Zhu, 2005) (Huang, Zhu, & Chang, 2007)
$Yxs(S) = \frac{a}{b + c \cdot e^{-dS}}$	(Sun et al., 2010)

Where S_i is the feed substrate concentration, in this case Carboxymethyl-cellulose (CMC), (Kg m^{-3}); S is the substrate concentration in the reaction mixture (Kg m^{-3}); X is the biomass concentration (Kg m^{-3}). In this contribution the specific growth rate μ, (h^{-1}) is a function μ: [0,S_{max}] → R with the following properties: i) μ is a differentiable function in the domain [0,Smax]. ii) $\mu(0) = 0$, and iii) $\mu(S) \leq \bar{\mu}_{max}$, where $\bar{\mu}_{max}$ is a scalar providing the upper bound of μ; D is the dilution rate (h^{-1}); Y is the biomass yield, ($Kg_{biomass}$ $Kg_{CMC^{-1}}$). S,X,D,Y $\in \mathbb{R}^+$. Biologically the initial conditions for the biomass and substrate concentrations at each time are: $X_0(t), S_0(t) \geq 0; t \in [0, \infty)$.

It is proposed that the biomass yield takes the form:

$$Y(S) = \left(\frac{1}{\alpha\sqrt{2\pi}}\right) e^{\left(\frac{-(S-\beta)^2}{2\alpha^2}\right)} \tag{3}$$

Which is a Gaussian type function. This proposed yield is supported by the behavior of the biomass and the substrate in the batch fermentations where the substrate inhibition takes place, from this, it can be noticed that at low substrate concentrations, less than the substrate inhibition concentration, the cellular yield increases, whereas at higher substrate concentrations the cellular yield decreases (Fig. 1). The Gaussian-type function is a realistic approach to describe the behavior of the cellular yield, where an important feature is that this model is bounded to the maximum cellular yield and can be extrapolated to several operation conditions, which is not the case for other biomass yield models as the linear and exponential functions.

There exists only a handful of biomass yield functions reported in literature (Table 2); all of them are function of the substrate or product concentrations. These proposals must satisfy that: I. $Y(0) \geq 0$,and $Y'(S) \geq 0, \forall [S_0^+, S^+]$. And the yield functions represent minimally the maintenance energy requirements, cell quota, mass energy balance, changes in the metabolic route or the enzymatic activity, cellular division, changes in cell morphology and age of culture (Pilyugin & Waltman, 2003).

3 On the local stability for the chemostat model

To assess the local stability of the equilibrium for the chemostat model, eqs. (1)-(2), it is used the Jacobian (J) linearization method. The stability characteristics are listen in Table 3.

3.1 Constant biomass yield

The local stability for the chemostat model with constant biomass yield has been reported in (Crooke *et al.* 1980). Following their key results:

$$J = \begin{bmatrix} -D - \frac{x\mu'(S)}{Y} & -\frac{\mu(S)}{Y} \\ x\mu'(S) & -D + \mu(S) \end{bmatrix} \tag{4}$$

Table 3. Local Stability Classification (Gray & Scoot, 1990).

Tr (J)	Det (J)	$Tr(J)^2$ -4Det(J)	$\lambda_{1,2}$	Stability characteristics
-	+	+	Real, both (-)	Stable Node
-	+	-	Complex, real part (-)	Stable Focus
0	+	-	Imaginary, real part =0	Hopf Bifurcation
+	+	-	Complex, real part (+)	Unstable Focus
+	+	+	Real, both (+)	Unstable Node
±	0	+	One zero, one (-) o (+)	Saddle-Node Bifurcation
±	-	+	Real, one (-) one (+)	Saddle Point
0	0	0	Both zero	Double zero Bifurcation Point

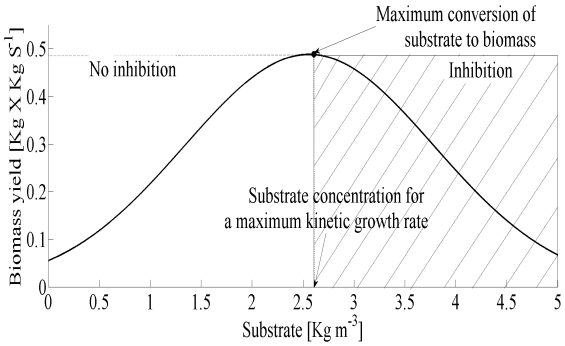

Fig. 1. Nonlinear biomass yield as a Gaussian type function.

Eq. (4) points out the linearization of the chemostat model considering the *biomass yield constant*. Considering that the chemostat achieves the so-called operational steady state in which $f(S^*,X^*) = 0; g(S^*,X^*) = 0 | S^*,X^* > 0 \Rightarrow D = \mu(S^*)$, the matrix can be reduced as:

$$J = \begin{bmatrix} -D - \frac{x\mu'(S)}{Y} & -\frac{\mu(S)}{Y} \\ x\mu'(S) & 0 \end{bmatrix} \tag{5}$$

The trace $Tr[J]$, determinant $Det[J]$, and discriminant $Dcr[J]$ values of Jacobian matrix provide information about the steady state stability for the chemostat model, eqs. (6)-(8):

$$Tr[J] = -\left(D + \frac{x\mu'(S)}{Y}\right) \tag{6}$$

$$Det[J] = \frac{x\mu'(S)D)}{Y} \tag{7}$$

$$Dcr[J] = \left(D - \frac{x\mu'(S)}{Y}\right)^2 \tag{8}$$

The $Tr[J]$, $Det[J]$, and $Dcr[J]$ analysis enclosed in Table 4 indicates that the chemostat model has a dichotomy, it can only show stable node and saddle point character stabilities $\Leftrightarrow [S,X,D,Y] \in \mathbb{R}^+$.

The same results are obtained with the eigenvalues:

$$\lambda_1 = -D \tag{9}$$

$$\lambda_2 = -\frac{x\mu'}{Y} \tag{10}$$

From eqs. (9)-(10), the chemostat model is *stable* $\forall D > 0 \wedge \mu'(S) > 0$ (as stable node) and unstable $\forall D > 0 \wedge \mu'(S) < 0$ (as saddle point) $\Leftrightarrow [S,X,D,Y] \in \mathbb{R}^+$.

3.2 *Variable biomass yield*

Now, if the biomass yield is a function of the substrate concentration, the Jacobian takes the form:

$$J = \begin{bmatrix} -D - X\gamma' & -\gamma \\ X\mu'(S) & -D + \mu(S) \end{bmatrix} \tag{11}$$

Where: $\gamma = \frac{\mu(S)}{Y}$ and $\gamma' = \frac{\mu'(S)Y - \mu(S)Y'}{Y^2}$. At the operational steady state $D = \mu(S)$, so eq. (11) is reduced to be:

$$J = \begin{bmatrix} -D - X\gamma' & -\gamma \\ X\mu'(S) & 0 \end{bmatrix} \tag{12}$$

Where:

$$Tr(J) = -(D + X\gamma') \tag{13}$$

$$Det(J) = X\mu'(S)\gamma \tag{14}$$

$$Dcr(J) = (-(D + X\gamma'))^2 - 4X\mu'(S)\gamma \tag{15}$$

Also, in the equilibrium: $X = (S_i - S)/Y$; with S is a positive solution of $\mu(S) - D = 0$. Then, eqs. (13)-(15) can be rearranged as follows:

$$Tr(J) = -\left(D + \frac{(S_i - S)\gamma'}{Y}\right) \tag{16}$$

$$Det(J) = \frac{[(S_i ?S)\mu'(S)\mu(S)]}{Y^2} \tag{17}$$

$$Dcr(J) = \left[-(D + \frac{(S_i - S)\gamma'}{Y}\right]^2 - \frac{4[(S_i - S)\mu'(S)\mu(S)]}{Y^2} \tag{18}$$

Table 4. Intervals where Tr[J], Det[J] and Dcr[J] can take positive, negative or cero values.

Value	$Tr(J)$	$Det(J)$	$Dcr(J)$
Positive	$-\left(D+\frac{x\mu'(S)}{Y}\right)>0 \Leftrightarrow$ $\mu'(S)<0 \wedge \left\|\frac{x\mu'(S)}{Y}\right\|>D$	$\frac{x\mu'(S)D}{Y}>0 \Leftrightarrow \mu'(S)>0$	$\left(D-\frac{x\mu'(S)}{Y}\right)^2>0 \forall$ $D \wedge \mu'(S)$
Negative	$-\left(D+\frac{x\mu'(S)}{Y}\right)<0 \Rightarrow \mu'(S)>-DY/x$	$\frac{x\mu'(S)D}{Y}<0 \Leftrightarrow \mu'(S)<0$	$\left(D-\frac{x\mu'(S)}{Y}\right)^2<0$ *Inexistence case*
Zero	$-D-\frac{x\mu'(S)}{Y}=0 \Leftrightarrow \mu'(S)=-DY/x$	$\frac{x\mu'(S)D}{Y}=0 \Rightarrow \mu'(S)=0 \wedge \vee$ $D=0$	$\left(D-\frac{x\mu'(S)}{Y}\right)^2=0 \Leftrightarrow$ $\frac{x\mu'(S)}{Y}=D$

Restrictions: $D, x\ y\ Y \in \Re^+$

The eqs. 16-18 associated with the criteria given in Table 3 indicates that the system could exhibit oscillations depending of the sign taken by γ' and $\mu'(S)$. In global terms, the bioreactor's stability depends of the microorganism´s metabolism (kinetic growth rate and biomass yield) and some operative parameters (the dilution rate (D) and the substrate concentration fed (S_i)).

4 Results and discussion

The numerical bifurcation analysis for the chemostat model was done in Matcont v.5.0, a free MATLAB? package for numerical bifurcation analysis of ODE mathematical models. The dilution rate and the substrate feeding were taken as the bifurcation parameters. This fact obeys the structure of the vector field (Lara-Cisneros *et al*. 2012). Some particular equilibrium points were chosen from the above bifurcation analysis to illustrate their trajectories, attraction domains and stabilities, through the construction of phase portraits, using *pplane8*, a MATLAB package for numerical analysis of ODEs.

4.1 Constant biomass yield

The results of the *Bifurcation Analysis* took place with the assembly of bifurcation diagrams, for this analysis, plotting the biomass concentration at different dilution rates (bifurcation parameter). These bifurcation diagrams were built-up for all the unstructured kinetic models in Table 1, with the exception of Moser model, because this model does not predicts steady state concentrations. Also, the bifurcation diagrams were constructed for four substrate feed concentrations, (S_i = 2, 4, 8 and 12 Kg m^{-3}). In the work of Agarwal *et al*. (2009) is reported that the biomass yield has different constant values for each substrate feed concentration.(Y = 0.61(S_i = 2), 0.36 (S_i = 4), 0.10 (S_i = 8) and 0.07 (S_i = 12) Kg$_{biomass}$ Kg$_{CMC^{-1}}$), these experimental results were taken into account in the bifurcation analysis. The initial conditions for CMC and biomass (S_0, X_0) are 0.1 and 1.44 Kg m^{-3}, respectively.

In Fig. 2 (left hand) is shown, the bifurcation diagrams for each unstructured model. Some critical points were marked in the diagrams; these were Branch Point 1 (*BP*1), Branch Point 2 (*BP*2) and Limit Point (*LP*), which represent biomass concentration in batch culture, washout condition (trivial solution) and maximum operating dilution rate, respectively. The equilibrium points from *BP*1 to *LP* are stable nodes, while those from *LP* to *BP*2 are saddle points, this last interval corresponds to a multiplicity steady state region.

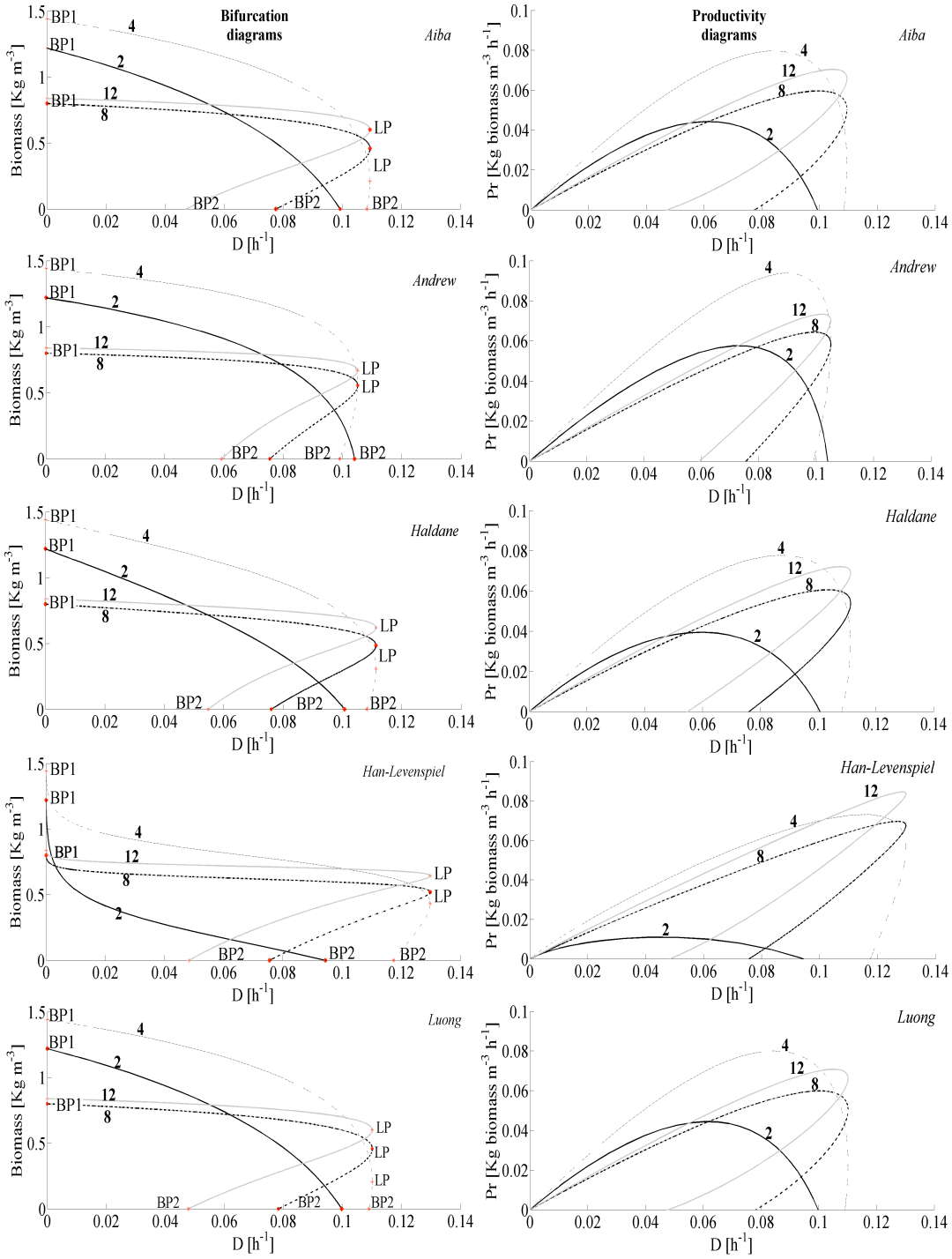

Fig. 2. Bifurcation diagrams (*left*) at Si, 2, 4, 8 & 12 Kg m^{-3}; and Y, 0.61, 0.36, 0.10, 0.07 $Kg_{biomass}$ $Kg_{CMC^{-1}}$ respectively, where BP1 (batch culture condition) and BP2 (washout condition) and LP (maximum operating dilution rate) are indicated. Productivity diagrams (*right*) at the same S_i and Y; for Aiba, Luong, Han-Levenspiel, Haldane and Aiba models.

For values equal to or greater than S_i = 4 Kg m^{-3} some similarities arisen between the bifurcation diagrams, as the steady state multiplicity appearance, where stable monotone solutions coexist with unstable monotone solutions, which represents a high risk in the operation of the bioreactor; the multiplicity interval increases with the increment of S_i; the hysteresis phenomenon is not predicted; neither oscillatory nor chaotic behavior.

On the other hand, there are some differences comparing the bifurcation diagram for Han-Levenspiel model with the other models, for example, the maximum operating dilution rate predicted by the Han-Levenspiel model (LP = 0.130 h^{-1}) is approximately 15% larger than the others and the steady state multiplicity interval for the Levenspiel model was larger than the rest of the models.

The Fig. 2 (right hand) shows the productivity diagrams. For all the models, with the exception of Han-Levenspiel model, the maximum biomass productivity ($Pr_m \approx$ 0.9 Kg m^{-3} h^{-1}) is reached at S_i = 4 Kg m^{-3} and a dilution rate around to 0.085 h^{-1} and for the Han-Levenspiel, the same productivity takes place at S_i = 12 Kg m^{-3} and a dilution rate approximately of 0.127 h^{-1} which is very close to the washout (D = 0.130 h^{-1}), also with the disadvantage of being in the multiplicity interval in contrast to other models, so, it is convenient to operate the reactor in other condition, a second option is S_i = 4 Kg m^{-3} and D = 0.115 h^{-1}, with a slightly lower productivity but neglected the multiplicity interval. Note that both operation conditions for Han-Levenspiel are outside of the operation range predicted with the other kinetic models.

In order to illustrate the trajectories, attraction domains and the stability, it was chosen the initial conditions: S_o = 8 Kg m^{-3}; X_o = 1.44 Kg m^{-3} and D = 0.09 h^{-1} to generate the corresponding phase portraits for each one of the unstructured kinetic models (Fig. 3). The steady state concentrations for biomass and substrate and their eigenvalues for the above initial conditions are shown in Table 5. In the phase portraits it is pointed out three equilibrium points (except Moser model), two of these are stable nodes and correspond to the trivial solution (TS) and nontrivial solution (NTS); the third point is a saddle point (SP), an unstable equilibrium, this in accordance with eqs. (6)-(8). It can be seen that all the trajectories below the saddle point converge to cell washout and those above the saddle point converge to an asymptotic stable node.

The Moser model is the only one that cannot present a NTS for any initial condition used, this is explained in Table 6, that shows for each model, their symbolic first derivative, analyzing the Moser model´s derivative, it is the only incapable to take positive values for any substrate concentration, therefore neglects the restrictions of eq. (10), which mentioned that the first derivate of μ regarding the substrate must be positive at least in a range of positive concentrations to reach a stable node. Similar results were reported by Fu *et al.* (2005), whom employing the Tissiet inhibition model and constant yield term for the chemostat model system found analytically and in simulations that the stability for the possible equilibrium points can only be stable node or saddle point.

Table 5. Eigenvalues and equilibrium points obtained for each kinetic growth model studied to the same initial conditions. Restriction: *Constant biomass yield*.

Unstructured kinetic model	R^2	*Initial condition*		D (h^{-1})	*Equilibrium point*		*Eigenvalues*		*Stability characteristics.*
		S_0 [Kg m^{-3}]	X_0 [Kg m^{-3}]		S [Kg m^{-3}]	X [Kg m^{-3}]	λ_1	λ_2	
Andrew´s	0.7450	8	1.44	0.09	1.102	0.6897	-0.2134	-0.09	Stable node
Luong´s	0.8215				1.554	0.6445	-0.1748	-0.09	Stable node
Han-Levenspiel	0.9393				1.961	0.6038	-0.7028	-0.09	Stable node
Haldane	0.8753				1.603	0.6396	-0.2107	-0.09	Stable node
Moser	0.7478				-	-	-	-	Not convergence
Aiba	0.8412				1.569	0.6430	-0.1706	-0.09	Stable node

Table 6. Unstructured models in study as well its first derivate with respect S.

Model	*Equation*	*First derivate with respect* S
Andrew´s	$\mu = \mu max \frac{S}{(Ks+S)(1+S/Ki)}$	$\mu' = \mu max \frac{1-\frac{S}{Ks+S}-\frac{S/Ki}{1+S/Ki}}{(Ks+S)(1+S/Ki)}$
Luong´s	$\mu = \mu max \frac{S}{(Ks+S)}\left(1-\frac{S}{S^u}\right)^n$	$\mu' = \mu max \frac{\left(1-\frac{S}{S^u}\right)^n\left[(Ks+S)\left[1-\frac{nS}{S^u}\left(1-\frac{S}{S^u}\right)^{-1}\right]-S\right]}{(Ks+S)^2}$
Han-Levenspiel	$\mu = \mu max \frac{\left(1-\frac{S}{Cs}\right)^n S}{S+Kl\left(1-\frac{S}{Cs}\right)^m}$	$\mu' = \mu max \frac{-\left(\frac{-(S-Cs)}{Cs}\right)^n\{Kl[(m-n-1)S+Cs]\left[\frac{-(S-Cs)}{Cs}\right]^m - nS^2\}}{(S-Cs)\left[Kl\left(\frac{-(S-Cs)}{Cs}\right)^m+S\right]^2}$
Haldane	$\mu = \mu max \frac{S}{\left(Ks+S+S^2/Ki\right)}$	$\mu' = \mu max \frac{Ks-S^2/Ki}{\left(Ks+S+S^2/Ki\right)^2}$
Moser	$\mu = \mu max \frac{S^n}{Ks+S^n}$	$\mu' = \mu max \frac{nKsS^n}{S(Ks+S^n)^2}$
Aiba	$\mu = \mu max \frac{S}{Ks+S} e^{-S/Ki}$	$\mu' = \mu max \frac{\left(1-\frac{S}{Ki}-\frac{S}{Ks+S}\right)e^{-S/Ki}}{Ks+S}$

4.2 Variable biomass yield

The bifurcation analysis with the variable biomass yield proposed was carried out with the same initial conditions reported in Section 4.1. Fig. 4 (left hand), shows the equilibrium branches for each kinetic model, where steady state multiplicity is predicted, as well as in the results for constant biomass yield, although the interval of multiplicity was reduced significantly. Critical points were marked, these were: Branch Point 1 (*BP*1), Branch Point 2 (*BP*2) and Limit Point (*LP*). Moreover, another critical point was found, the Hopf Bifurcation (*H*), indicating the appearance or disappearance of a limit cycle, meaning that sustained oscillations happen in the bioreactor. There exist a maximum of two Hopf bifurcation points for the same equilibrium branch (*H*1 and *H*2).

The phase portraits were constructed with the same initial conditions that yields the *H*1 (except Moser and Han-Levenspiel model) (Table 7), with the aim to show the trajectories and the attraction domain of the limit cycle (Fig. 5). To reveal the interval of D where the oscillations exist, the eigenvalues for the equilibrium branches were obtained and their imaginary part were plotted in Fig. 6. It is pointed out in Table 3 the eigenvalues with complex numbers that indicate oscillatory behavior (stable and unstable focus and Hopf bifurcation), also in the stability analysis showed in Section 3.2, it is proved that oscillatory behavior can exist, and it also depends explicitly of value S_i, eqs. (16)-(18). For this study model, the oscillations arose for the interval between $4 \leq S_i \leq 12$.

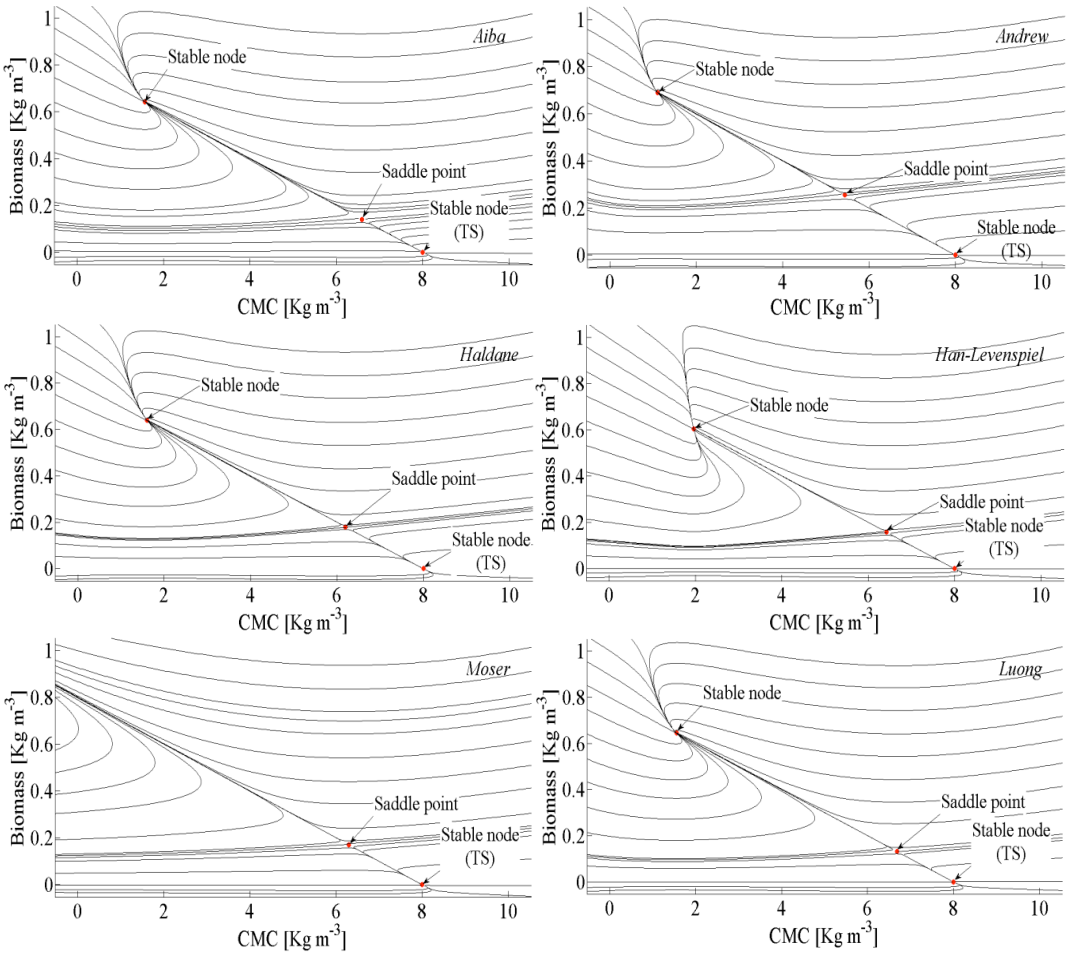

Fig. 3. Phase portrait´s for Andrew, Haldane, Han-Levenspiel, Luong, Moser & Aiba at D=0.09 h^{-1}; S0= 8 Kg m^{-3}; X_0=1.44 Kg m^{-3} and Y=0.10 Kgbiomass $Kg_{CMC^{-1}}$.

The simulations results with the kinetic rate laws listed in Table 1 (except Moser model) showed strong differences in the predictions of oscillatory behavior between them. The bifurcation diagram using the Han-Levenspiel´s model had the greatest differences compared to the other unstructured models. Some of these differences were that the location of the predicted equilibrium points change drastically in all the intervals of dilution rates studied; the intervals of oscillatory behavior is intensely reduced with the increment of S_i; the maximum operable dilution rate (*LP*) predicted was higher with Han-Levenspiel model than the other models.

The Hopf bifurcation points, $H1$ and $H2$, predicted only for the Aiba, Andrew, Haldane and Luong models, were characterized from the Lyapunov coefficients; the $H1$ is supercritical, meaning that is stable with small magnitude oscillations and it does not relies in the multiplicity region. This is in disagreement with the results of Pilyugin & Waltman (2003), that states that only supercritical bifurcations

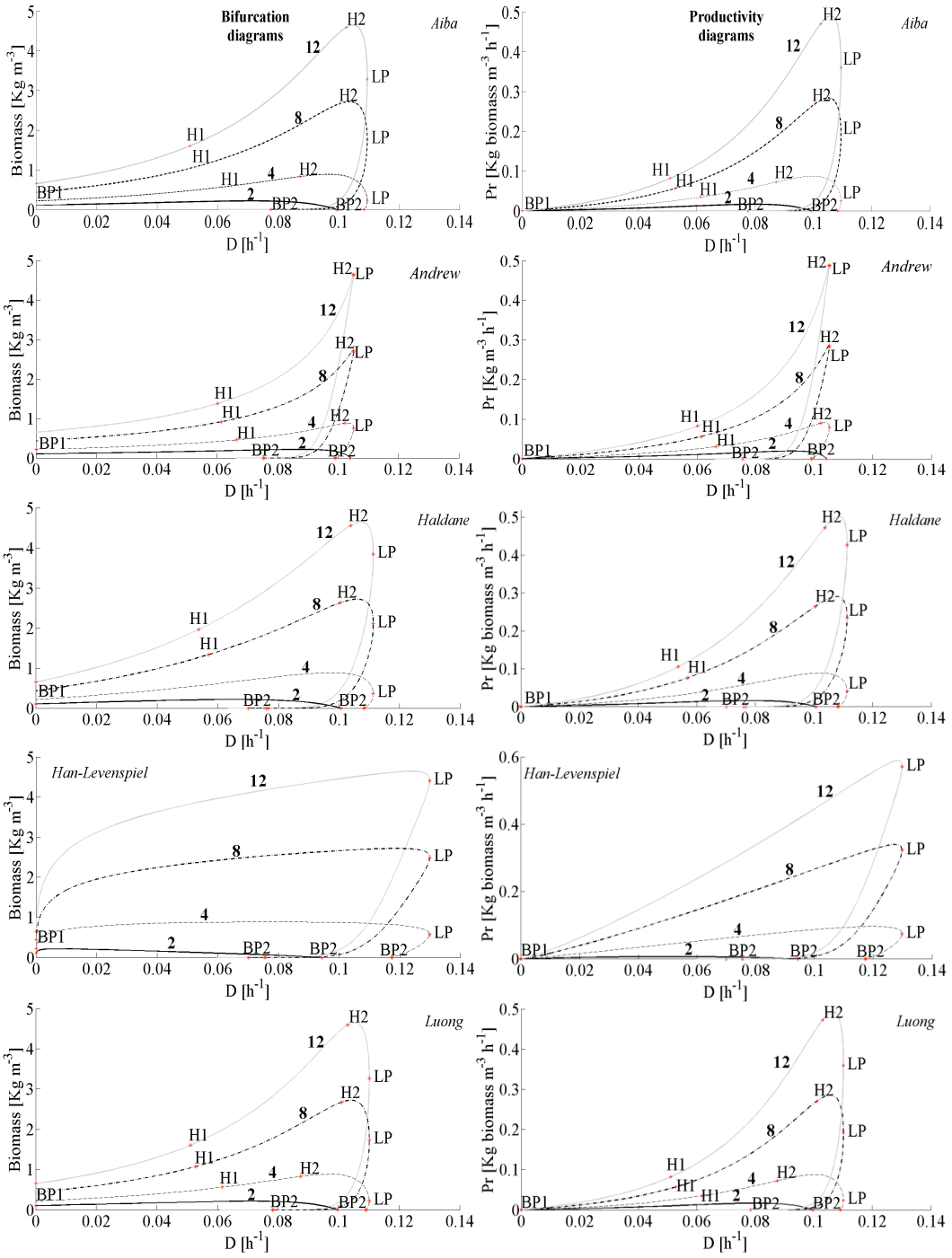

Fig. 4. Bifurcation diagrams (*left*) at Si, 2, 4, 8 & 12 Kg m^{-3}; and Y, as a Gaussian function $Kg_{biomass}$ $Kg_{CMC^{-1}}$ respectively, where BP1 (batch culture condition) and BP2 (washout condition) and LP (maximum operating dilution rate) are indicated. Productivity diagrams (*right*) at the same S_i and Y; for Aiba, Luong, Han-Levenspiel, Haldane and Aiba models.

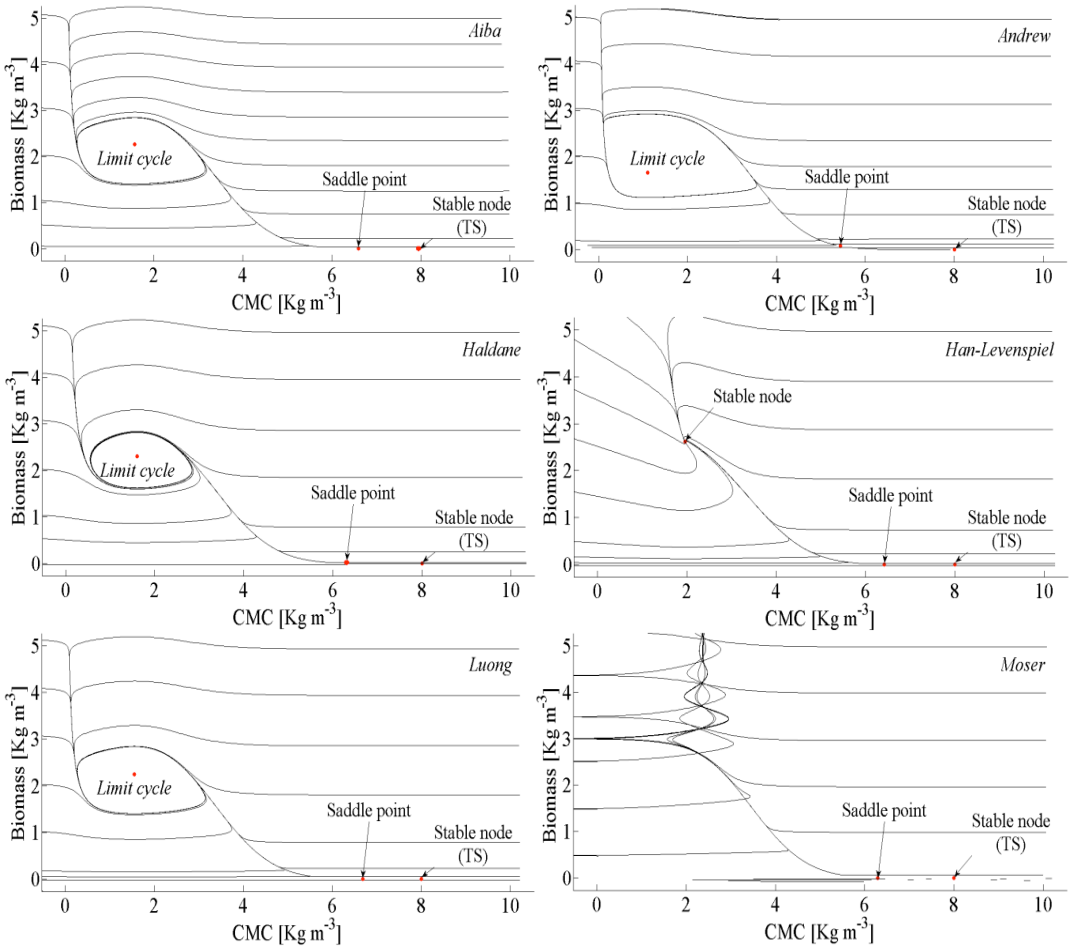

Fig. 5. Phase portrait´s for Andrew, Haldane, Han-Levenspiel, Luong, Moser & Aiba at D=0.09 h^{-1}; Si= 8 Kg m^{-3}; Xi=1.44 Kg m^{-3} and Y as a Gaussian function.

occur when the yield varies linearly with S. The $H2$ falls in the interval of multiplicity, it coexists with an unstable node, $H2$ is subcritical with high amplitude and period. Moreover, a new bifurcation analysis was carried out taking two bifurcation parameters, D and S_i (a 2-co-dimension bifurcation), starting from $H1$ to $H2$, where it was marked the conditions for the vanishing of the limit cycles (LPC). The Fig 7 gives information about the amplitude and the period of the oscillations, also, illustrates the family of limit cycles (loop of limit cycles) that lies in the state-parameter space studied. This loop showed a closed region, where only unstable periodic solutions are predicted and coexist with unstable nodes.

Concluding remarks

In this paper the dynamical behavior of a chemostat model has been analyzed by numerical bifurcation where the kinetic growth was described by a set or unstructured growth models and under the assumption that the biomass yield is constant, or a function of the substrate concentration. The variable yield model proposed here is of the form of a Gaussian-type function, and represent a more realistic approach to describe the behavior of the cellular yield. Significant changes in the chemostat behavior were obtained when the Gaussian yield function was used, instead the constant biomass yield value, as Hopf points prediction, differences in the steady state multiplicity intervals, productivity and equilibrium stability; and for the Han-Levenspiel growth model, that predicts

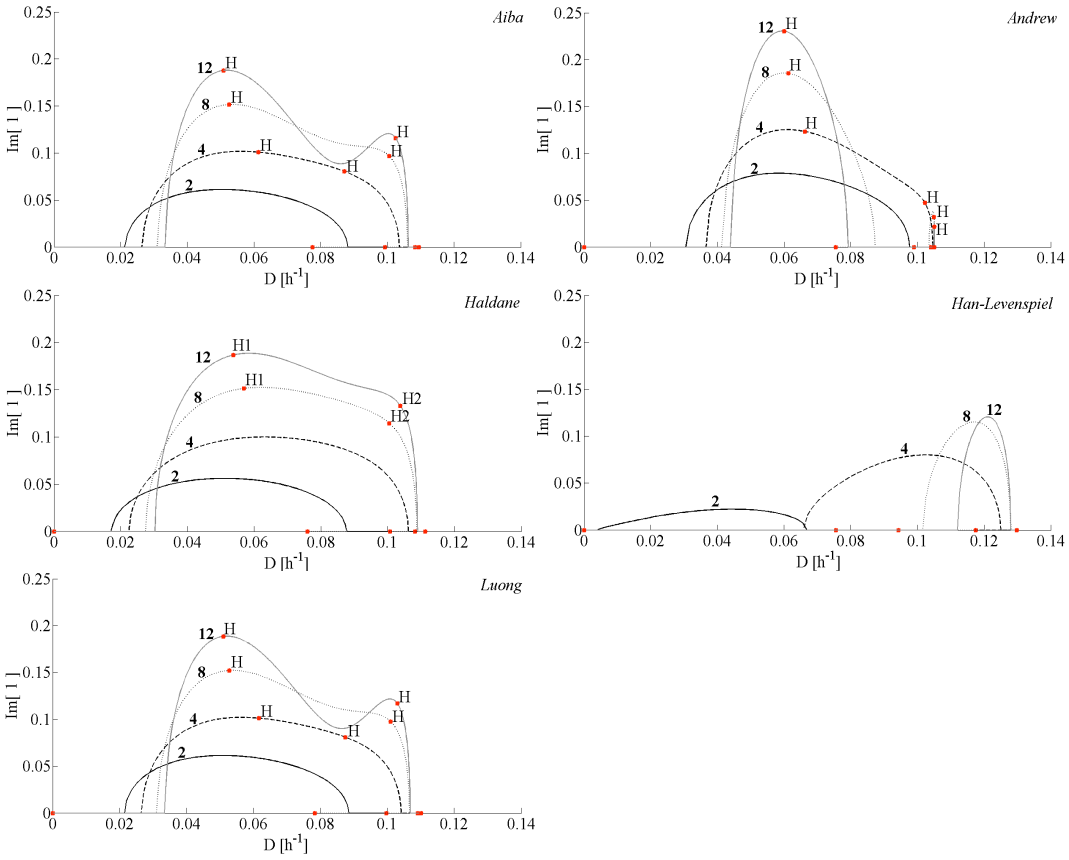

Fig. 6. Bifurcation diagrams at Si, 2, 4, 8 & 12 Kg m^{-3}; and *Y*, as a Gaussian function Kgbiomass $Kg_{CMC^{-1}}$ where it is shown the imaginary part of the complex eigenvalues that reveal the intervals where the system oscillates. It is only pointed the Hopf bifurcation (H).

Table 7. Eigenvalues and equilibrium points obtained for each kinetic growth model studied to the same initial conditions. Restriction: *Variable biomass yield*.

Unstructured kinetic model	R^2	*Initial condition*		D (h^{-1})	*Equilibrium point*		*Eigenvalues*		*Stability characteristics*
		So [Kg m^{-3}]	Xo [Kg m^{-3}]		S [Kg m^{-3}]	X [Kg m^{-3}]	λ_1	λ_2	
Andrew	0.7450	8	1.44	0.09	1.102	1.6561	-0.2134	-0.09	Nodal source
Luong	0.8215				1.554	2.2446	0.06241+ 0.10882*i*	0.06241- 0.10882*i*	Spiral source
Han-Levenspiel	0.9393				1.961	2.6153	-0.42735	-0.14802	Nodal sink
Haldane	0.8753				1.603	2.3006	0.03357+ 0.13356*i*	0.03357- 0.13356*i*	Spiral source
Moser	0.7478				-	-	-	-	Not convergence
Aiba	0.8412				1.569	2.2617	0.06121+ 0.10774*i*	0.06121- 0.10774*i*	Spiral source

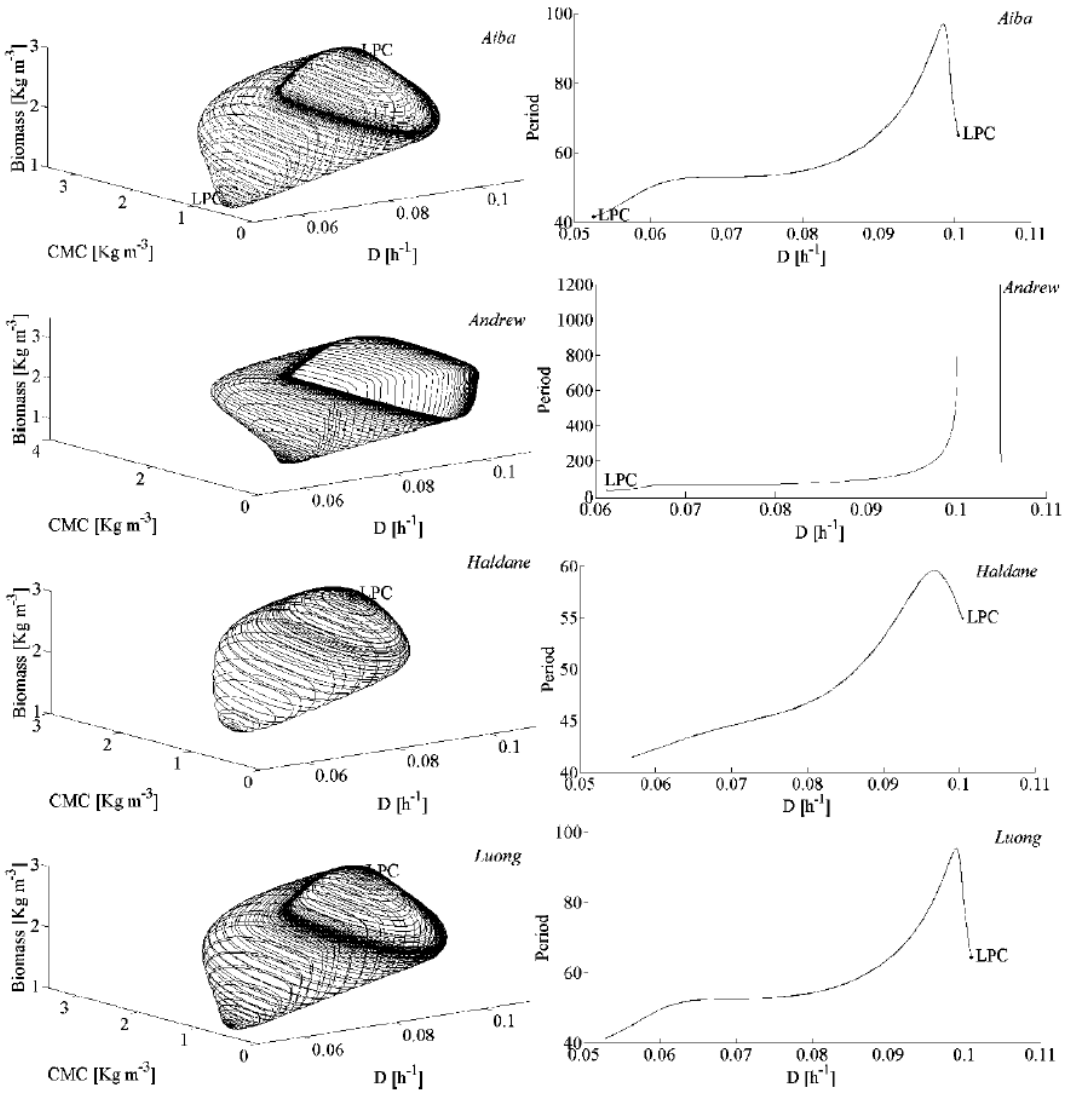

Fig. 7. Hopf bifurcation continuation with the Gaussian yield, Si=8 Kg m^{-3}. Left-hand the oscillations amplitude for CMC and biomass; right-hand, oscillations period between two Hopf bifurcations.

a maximum dilution rate over the other unstructured models and different equilibrium branches. The above results disclose that chemostat model predictions can vary greatly according to the unstructured growth model and the biomass yield. It also shows the necessity of the validation of simulation results with laboratory experiments to choose the most appropriate bioreactor model, thus leading to an improvement of the bioreactor design and control.

Acknowledgements

R.V.G.A wishes to acknowledge to the CINVESTAV and the CONACyT for the doctoral scholarship number 290564; Gerardo Lara-Cisneros thanks CONACyT for the postdoctoral fellowship grant.

Nomenclature

Si	Initial substrate concentration, Kg m^{-3}
S	Substrate concentration, Kg m^{-3}
D	Dilution rate, h^{-1}
X	Biomass concentration, Kg m^{-3}
Y	Biomass yield, Kgbiomass $KgCMC^{-1}$
X_o	initial biomass concentration, Kg m^{-3}
CMC	Carboxymethylcellulose
Pr_m	maximum biomass productivity
LP	Limit Point
LPC	Limit Point Cycle
BP_n	Branch Point n
H_n	Hopf n
N	Neutral Saddle
TS	Trivial solution
Im [n]	Imaginary number [n]

Greek symbols

μ	Specific growth rate, h^{-1}
μ'	First derivate with respect to the substrate for specific growth rate
λ_n	Eigenvalues

References

Abashar, M. y Elnashaie, S. (2010). Dynamic and chaotic behavior of periodically forced fermentors for bioethanol production. *Chemical Engineering Science 65*, 4894.

Agarwal, R., Mahanty, B. y Dasu, V.V. (2009). Modeling growth of *Cellulomonas cellulans* nrrl b 4567 under substrate inhibition during cellulase production. *Chemical and Biochemical Engineering Quarterly 23*, 213.

Agrawal, P., Lee, C., Lim, H.C. y Ramkrishna, D. (1982). Theorical investigations of dynamic behavior of isothermal continuous stirred tank biological reactors. *Chemical Engineering Science 37*, 453.

Ajbar, A. (2001). On the existence of oscillatory behavior in unstructered models of bioreactors. *Chemical Engineering Science 56*, 1991.

Ajbar, A. y Alhumaizi, K. (2012). *Dynamics of the chemostat : A bifurcation theory approach*. CRC Press Taylor & Francis Group, USA.

Alvarez-Ramirez, J., Alvarez, J. y Velasco, A. (2009). On the existence of sustained oscillations in a class of bioreactors. *Computers & Chemical Engineering 33*, 4.

Allen, L.J.S. (2007). *An Introduction to Mathematical Biology*. Pearson/Prentice Hall, NJ.

Crooke, P.S., Wei, C.-J. y Tanner, R.D. (1980). The effect of the specific growth rate and yield expressions on the existence of oscillatory behavior of a continuous fermentation model. *Chemical Engineering Communications 6*, 333.

Dong, Q.L. y Ma, W.B. (2013). Qualitative analysis of the chemostat model with variable yield and a time delay. *Journal of Mathematical Chemistry 51*, 1274.

Fu, G. y Ma, W. (2006). Hopf bifurcations of a variable yield chemostat model with inhibitory exponential substrate uptake. *Chaos, Solitons & Fractals 30*, 845.

Fu, G., Ma, W. y Shigui, R. (2005). Qualitative analysis of a chemostat model with inhibitory exponential substrate uptake. *Chaos, Solitons & Fractals 23*, 873.

Garhyan, P., Elnashaie, S.S.E.H., Al-Haddad, S.M., Ibrahim, G. y Elshishini, S.S. (2003). Exploration and exploitation of bifurcation/chaotic behavior of a continuous fermentor for the production of ethanol. *Chemical Engineering Science 58*, 1479.

Gray, P. y Scoot, S.K. (1990). *Chemical oscillations and instabilities. Non-linear chemical kinetic*. Clarendon Press. Oxford,

Huang, X., Zhu, L. y Chang, E.H.C. (2007). Limit cycles in a chemostat with general variable yields and growth rates. *Nonlinear Analysis: Real World Applications 8*, 165.

Ibrahim, G., Habib, H. y Saleh, O. (2008). Periodic and chaotic solutions for a model of a bioreactor with cell recycle. *Biochemical Engineering Journal 38*, 124.

Karaaslanl, C.Ç. (2012) Bifurcation analysis and its applications. En: *Numerical simulation - from theory to industry*, (M. Andriychuk,ed.), Pp. 3. Intech.

Lara-Cisneros, G., Femat, R. y Perez, E. (2012). On dynamical behaviour of two-dimensional biological reactors. *International Journal of Systems Science 43*, 526.

Lenbury, Y. y Chiaranai, C. (1987). Bifurcation analysis of a product inhibition model of a continuous fermentation process. *Applied Microbiology and Biotechnology 25*, 532.

Lenbury, Y.W. y Punpocha, M. (1989). The effect of the yield expression on the existence of oscillatory behavior in a three-variable model of a continuous fermentation system subject to product inhibition. *Biosystems 22*, 273.

Namjoshi, A., Kienle, A. y Ramkrishna, D. (2003). Steady-state multiplicity in bioreactors: Bifurcation analysis of cybernetic models. *Chemical Engineering Science 58*, 793.

Nelson, M.I. y Sidhu, H.S. (2005). Analysis of a chemostat model with variable yield coefficient. *Journal of Mathematical Chemistry 38*, 605.

Nelson, M.I. y Sidhu, H.S. (2008). Analysis of a chemostat model with variable yield coefficient: Tessier kinetics. *Journal of Mathematical Chemistry 46*, 303.

Nelson, M.I., Sidhu, H.S. (2009). Analysis of a chemostat model with variable yield coefficient: Tessier kinetics. *Journal of Mathematical Chemistry 46*, 303.

Nielsen, J.H., Villadsen, J. y Lide?n, G. (2003). *Bioreaction Engineering Principles* (3rd. ed.). Springer. New York.

Pilyugin, S.S.W., Paul. (2003). Multiple limit cycles in the chemostat with variable yield. *Mathematical Biosciences 182*, 151.

Gupta, P., Samant, K., and Sahu, A. (2012). Isolation of cellulose-degrading bacteria and determination of their cellulolytic potential. *International Journal of Microbiology 2012*, 1.

Sterner, R.W., Small, G. E. & Hood, J. M. (2012). The conservation of mass. *Nature Education Knowledge 3*, 20.

Strogatz, S.H. (1994). *Nonlinear dynamics and chaos : With applications to physics, biology, chemistry, and engineering*. Perseus Books Publishing, L.L.C. Massachusetss, U.S.

Sun, J.-Q. y Luo, A.C.J. (2012). *Global Analysis of Nonlinear Dynamics*. Springer, New York.

Sun, K., Tian , Y., Chen, L. y Kasperski, A. (2010). Nonlinear modelling of a synchronized chemostat with impulsive state. *Mathematical and Computer Modelling 52*, 227.

Wu, W., & Chang, H.-Y. (2007). Output regulation of self-oscillating biosystems: Model-based pi/pid control approches. *Industrial & Engineering Chemistry Research*.

Zhang, Y. & Henson, M.A. (2001). Bifurcation analysis of continuous biochemical reactor models. *Biotechnology Progress 17*, 647.

Appendix A

Bifurcation theory

The objective of bifurcation theory is to characterize changes in the qualitative dynamic behavior of a nonlinear system as the key parameter values (for example, coefficients of a reaction rate) are changed (Zhang & Henson, 2001). This means that the system achieves a critical parameter value, where an orbit change occurs and, as a consequence, the possibility of different stability properties of equilibrium; if this qualitative change does not occur and a quantitatively different behavior is only present, the system is structurally stable (Karaaslanl, 2012). Formally, Bifurcation can be introduced as follows:

The appearance of a topologically nonlinear phase portrait under variation of a parameter is called a bifurcation (Zhang & Henson, 2001).

A more efficient and complete characterization of the model behavior that are difficult to ascertain simply integrating the model equations over time are disclosed through the bifurcation analysis (Zhang & Henson, 2001; Garhyan *et al*. 2003), therefore, it is a way to validate if the models supports the steady state and dynamic behavior observed experimentally; it is a powerful method to search the parameters' values, where oscillations exist and to discretize between models that present high correlation with experimental data. This analysis can be used to fix intervals of bioreactor operation and to keep the bioreactor away from undesirable steady states and direct it towards more beneficial ones. (Zhang & Henson, 2001; Namjoshi *et al*. 2003).

There are two types of bifurcations, local and global, the first correspond to the analysis through local stability properties of the equilibria by computing Taylor's series expansion of the state

space model. Local bifurcation occurs when some of the eigenvalues approach the imaginary axis in the complex plane. The simplest bifurcations are associated with a single real eigenvalue becoming zero ($\lambda_1 = 0$) (Fold bifurcation) as the case of Branch Point (BP) and Limit Point (LP) or a pair of complex conjugate eigenvalues crossing the imaginary axis ($\lambda_{1,2} = \pm i\gamma$, $\gamma > 0$) namely Hopf point (H), the saddle point appears when the eigenvalues are strictly real numbers with opposite signs ($\lambda_1 = -R$, $\lambda_2 = R$). Fold bifurcations usually are the cause of multiple steady states and hysteresis behavior. Hopf bifurcations are responsible for the appearance and disappearance of periodic solutions (Limit cycles) (Zhang & Henson, 2001). The local bifurcations are listed in Table 3. The second refers to some large invariant sets of the system that collide with each other, or with equilibria of the system. The simplest global bifurcations correspond to the creation or destruction of a *homoclinic* or *heteroclinic orbit*, for which no local information is sufficient. A homoclinic orbit connects equilibrium to itself, whereas a heteroclinic orbit refers to connecting two different equilibria.

Limit cycles could be detected through the Hopf bifurcation as is indicated in following theorem:

Theorem 1. Hopf bifurcation theorem. Consider the autonomous invariant system:

$$\frac{ds}{dt} = f(s, x, D); \frac{dx}{dt} = g(s, x, D) \qquad \text{(A.1)}$$

Where the functions f and g, depend on the bifurcation parameter D. Suppose there exist an equilibrium $(\bar{s}(D), \bar{x}(D))$ of system (A.1) and the Jacobian matrix evaluated at this equilibrium has eigenvalues $\alpha(D) \pm i\beta(D)$. In addition, suppose a change in stability occurs at the value of $D = D^*$, where $\alpha(D^*) = 0$. If $\alpha(D) < 0$ for values of r close to D^* but for $D < D^*$ and if $\alpha(D) > 0$ for values of D close to D^* but for $D > D^*$ (also $\beta(D^*) \neq 0$)), then the equilibrium changes from the stable spiral to an unstable spiral as r passes through D^*. The Hopf bifurcation theorem indicates that there exists a periodic orbit near $D = D^*$ for any neighborhood of the equilibrium in $\mathbb{R}^2$. The parameter D is the bifurcation parameter and D^* is the bifurcation value. The theorem is valid only when the bifurcation parameter has values close to the bifurcation value (Allen, 2007).

At the Hopf bifurcation, as D passes through the bifurcation value $D*$, there are three possible dynamics that may occur:

(i) At the bifurcation parameter $D*$ infinitely many neutrally stable concentric closed orbits encircle the equilibrium.

(ii) A stable spiral changes to a stable limit cycle for values of the parameter close to $D*$ (supercritical bifurcation).

(iii) A stable spiral an unstable limit cycle change to an unstable spiral for values of the parameters close to $D*$ (subcritical bifurcation) (Ajbar, 2001; Allen, 2007).